Journal of Physiology (2002), **543.3**, *pp.* 899–916
DOI: 10.1113/jphysiol.2002.019703

www.jphysiol.org

Journal of Physiology

The scotopic threshold response of the dark-adapted electroretinogram of the mouse

Shannon M. Saszik, John G. Robson and Laura J. Frishman

College of Optometry, University of Houston, Houston, TX 77204-2020, USA

The most sensitive response in the dark-adapted electroretinogram (ERG), the scotopic threshold response (STR) which originates from the proximal retina, has been identified in several mammals including humans, but previously not in the mouse. The current study established the presence and assessed the nature of the mouse STR. ERGs were recorded from adult wild-type C57/BL6 mice anaesthetized with ketamine (70 mg kg^{-1}) and xylazine (7 mg kg^{-1}). Recordings were between DTL fibres placed under contact lenses on the two eyes. Monocular test stimuli were brief flashes (λ_{max} 462 nm; −6.1 to +1.8 log scotopic Troland seconds(sc td s)) under fully dark-adapted conditions and in the presence of steady adapting backgrounds (−3.2 to −1.7 log sc td). For the weakest test stimuli, ERGs consisted of a slow negative potential maximal ~200 ms after the flash, with a small positive potential preceding it. The negative wave resembled the STR of other species. As intensity was increased, the negative potential saturated but the positive potential (maximal ~110 ms) continued to grow as the b-wave. For stimuli that saturated the b-wave, the a-wave emerged. For stimulus strengths up to those at which the a-wave emerged, ERG amplitudes measured at fixed times after the flash (110 and 200 ms) were fitted with a model assuming an initially linear rise of response amplitude with intensity, followed by saturation of five components of declining sensitivity: a negative STR (nSTR), a positive STR (pSTR), a positive scotopic response (pSR), PII (the bipolar cell component) and PIII (the photoreceptor component). The nSTR and pSTR were approximately 3 times more sensitive than the pSR, which was approximately 7 times more sensitive than PII. The sensitive positive components dominated the b-wave up to > 5 % of its saturated amplitude. Pharmacological agents that suppress proximal retinal activity (e.g. GABA) minimized the pSTR, nSTR and pSR, essentially isolating PII which rose linearly with intensity before showing hyperbolic saturation. The nSTR, pSTR and pSR were desensitized by weaker backgrounds than those desensitizing PII. In conclusion, ERG components of proximal retinal origin that are more sensitive to test flashes and adapting backgrounds than PII provide the 'threshold' negative and positive (b-wave) responses of the mouse dark-adapted ERG. These results support the use of the mouse ERG in studies of proximal retinal function.

(Received 27 February 2002; accepted after revision 20 June 2002; first published online 26 July 2002)
Corresponding author L. J. Frishman: College of Optometry, University of Houston, 505 J Davis Armistead Building, Houston, TX 77204-2020, USA. Email: lfrishman@uh.edu

The flash electroretinogram (ERG) is a useful tool for assessing retinal function in both the laboratory and the clinic. It is a mass electrical potential that changes in a characteristic way in response to an increase in retinal illumination, and it can be recorded non-invasively using a corneal electrode. Recording non-invasively provides the opportunity for studying retinal function while maintaining an essentially normal physiological environment for the tissue. However, because it is a mass potential, the ERG represents the summed activity of all retinal cells. For specific information about retinal function, it is important to be able to separately analyse the contributions from the cells and circuits that combine to form the mass response.

Much research on the flash ERG has focused on separating the various components of the response that correspond to different retinal cell types. As a result, it is well known that the initial waves of the dark-adapted (scotopic) ERG, the a- and b-waves, originate mainly from cells at early stages of retinal processing. Following an intense brief flash of light from darkness, the negative-going a-wave is generated by rod photocurrents (Penn & Hagins, 1969) and the positive-going b-wave by depolarizing bipolar-cell currents in combination with bipolar cell-dependent K^+ currents affecting Müller cells (Miller & Dowling, 1970; Stockton & Slaughter, 1989; Xu & Karwoski, 1994; Shiells & Falk, 1999; Robson & Frishman, 1995, 1999; for a review see Pugh *et al.* 1998). For weaker flashes, the a-wave is too small to be seen in the record, and the dominant component of the ERG is the b-wave.

For very weak flashes from darkness, in several mammals, e.g. cats, monkeys, humans, and rats, a small post-

receptoral potential of opposite polarity to the b-wave dominates the ERG (Sieving *et al.* 1986; Sieving & Nino, 1988; Sieving & Wakabayashi, 1991; Bush & Remé, 1992). This negative-going response, which is more sensitive than the scotopic b-wave, and saturates at a lower light level, has been called the scotopic threshold response (STR). The STR is generated more proximally in the retina than the b-wave (Sieving *et al.* 1986; Frishman & Steinberg, 1989*a*,*b*; Naarendorp & Sieving, 1991), and is thought to reflect activity of the proximal retinal, i.e. amacrine and ganglion cell, portion of the sensitive rod circuit that is specialized for handling quantal events.

The STR has also been shown to be more sensitive to the effects of background light than the b-wave, which, in turn is more sensitive than the a-wave (Frishman & Sieving, 1995). Because the STR is desensitized by backgrounds that are too weak to affect the sensitivity of the b-wave or the a-wave, it is likely that the cellular mechanisms for the 'network' adaptation of the STR reside in inner retina. At present, these mechanisms are not well understood.

The ERG is a valuable tool for assessing the function of retinal cells and circuits *in vivo*. The development of the ability to genetically alter retinas in murine models has provided new opportunities for studying retinal processing. Although the STR could be useful in studies of inner retinal circuits, and the mechanisms of network adaptation in mice, it has not yet been characterized in this species. The purpose of the present study was to determine whether the STR is present in the mouse retina, and the extent to which it shares the characteristics observed in other species. In this study we found that, as in other species, the mouse STR, which is more clearly composed of both positive and negative components, is the most sensitive portion of the ERG. It originates from the inner retina proximal to bipolar cells, and is exquisitely sensitive to background lights. We also provide evidence for another proximal retinal component of positive polarity that is slightly less sensitive that the STR, but more sensitive than the portion of the b-wave that is produced by bipolar cells. Results from this study have appeared previously in abstract form (Saszik *et al.* 2001).

METHODS

Subjects

Subjects were adult C57/BL6 mice between 2 and 6 months old (Simonsen Lab, Gilroy, CA, USA). The mice were reared and housed in a room with a 14 h light (<40 lux)–10 h dark cycle. The experimental procedures adhered to the ARVO Statement for the Use of Animals in Ophthalmic and Vision Research and were approved by the Institutional Animal Care and Use Committee of the University of Houston.

General procedures

ERG recording. Animals were dark-adapted overnight and prepared for recording under red illumination (LED, $\lambda > 620$ nm). They were anaesthetized initially with an I.P. injection of ketamine (70 mg kg^{-1}; Vedco, Inc., St Joseph, MO, USA) and xylazine (7 mg kg^{-1}; Vedco), and anaesthesia was maintained with ketamine (72 mg kg^{-1}) and xylazine (5 mg kg^{-1}) every 45 min via a subcutaneous needle fixed in the flank. Pupils were dilated to 3 mm in diameter with topical atropine (0.5 %) and phenylephrine (2.5 %). Rectal temperature was monitored and maintained between 37 and 38 °C with an electrically heated blanket (CWE, Inc., Ardmore, PA, USA). The animal's head was stabilized by drawing the nose into a small perforated plastic tube with a wire lasso hooked behind the upper teeth. This wire served as the earth wire. Recording sessions lasted from 4 to 8 h, and animals generally recovered from the anaesthesia after the session. Some animals were killed after recording sessions using an I.P. dose of sodium pentobarbitone (100 mg kg^{-1}).

ERGs were recorded differentially between DTL (Dawson *et al.* 1979) fibre electrodes placed on the two eyes, as used previously in studies of the dark-adapted ERG in monkeys (Frishman *et al.* 1996*b*) and humans (Frishman *et al.* 1996*a*). Each electrode was moistened with 1.2 % methylcellulose in 1.2 % saline and on the stimulated eye it was covered with a contact lens heat-formed from 0.2 mm clear ACLAR film (Honeywell, USA). The cornea of the non-stimulated eye was covered completely with an opaque contact lens formed from 0.7 mm rigid black PVC sheet. The signal was amplified (DC to 300 Hz), and after being digitized at 1 kHz with a resolution of 2 μV was sent to the computer for averaging, display and storage.

The stimulus consisted of brief full field flashes (LEDs; λ_{max}, 462 nm) either from darkness or in the presence of a variety of steady backgrounds from −3.2 to −1.7 log scotopic Trolands (sc td) provided by a separate set of LEDs, (λ_{max}, 462 nm). The ganzfeld stimulus was produced by rear illumination of a white diffuser (35 mm in diameter) positioned very close to one eye, tipped away from the non-stimulated eye. For the weak stimuli used in the present study, the possibility of light spill affecting the non-stimulated, covered eye either via the sclera or the skull, would be minimal. To check whether light leak in the non-stimulated eye affected ERG responses to the strongest stimuli, responses recorded using the covered eye as a reference were compared with responses referenced to a needle in the temple near the covered eye, or inserted between the eyes, and they were all similar. Test flash energy could be altered by choosing which of several differently attenuated LEDs to activate as well as by altering the duration of the current pulse applied to the LED (from 0.8 μs up to 4.1 ms). Time zero was taken to be half-way through the flash. The test flash energies used ranged, by successive doubling (i.e. at 0.3 log unit intervals), from stimuli too weak to produce measurable responses (−6.1 log sc td s) to very strong stimuli that elicited visible a-waves (>−0.5 log sc td s). The interval between flashes was adjusted so that responses returned to baseline before another stimulus was presented. For flash energies $\leqslant$ −2.6 log sc td s intervals were 1.5 s; >−2.6 and $\leqslant$ −1.5 log sc td s, 2 s; >−1.5 and $\leqslant$ 1.0 log sc td s, 3 s and intervals between flashes of higher energy than 1.0 log sc td s were 4 s. Responses were averaged over many trials when stimuli were weak and responses were small, and over fewer trials when responses were larger. In addition, three-point weighted smoothing (0.25, 0.5, 0.25) and a 60 Hz digital notch filter were used to reduce noise in the responses.

Intravitreal injections. A small hole was punctured in the eye just behind the limbus using a 30 gauge needle. Pharmacological agents, γ-aminobutyric acid (GABA) or *N*-methyl-D-aspartic acid (NMDA), were injected into the eye (~1–1.5 μl) through the

hole using a glass pipette (tip diameter ~20 μm) fixed on a 10 μl Hamilton Microsyringe (Hamilton Company, Reno, NV, USA). We chose injectate concentrations that produced concentrations in the vitreous humour (based on an estimated vitreal volume of 20 μl) similar to those used previously in cat (e.g. Naarendorp & Sieving, 1991; Robson & Frishman, 1995). After the injection the ERG was monitored until no further change was seen in the response. Responses usually recovered to full amplitude and became stable within 2 h.

Data analysis and modelling. Response amplitudes were measured at fixed times after stimulus flashes corresponding to the dominant positive peak (110 ms after the flash) and negative trough (200 ms) in the dark-adapted ERG, and plotted *vs.* stimulus energy. Based upon inspection of the raw data, examination of the observed amplitude–energy functions, and previous findings in other species (Robson & Frishman, 1995; Frishman *et al.* 1996*b*; Frishman & Robson, 1999) we fitted our amplitude–energy data with a model incorporating five components. The assumption was made that each component rose in proportion to stimulus energy for weak stimuli (i.e. in the linear response range) and then saturated according to one of three characteristic functions, specifically, a hyperbolic, exponential or a truncated ramp function (i.e. a function that is linear until it abruptly reaches the saturation level).

Modelling of amplitude–energy data measured at 110 and 200 ms was carried out in SigmaPlot 2000 and 2001 (SPSS) using this program's implementation of the Marquardt-Levenberg algorithm to find parameter values that minimized a weighted sum of the squared differences between the observed data and the predicted model. The same five components were used to model data measured at 110 and 200 ms after the stimulus flash. For a given animal, certain model parameters were common to measurements made at the two times, whereas others were allowed to differ (see Results for details of the modelling). In all cases the correlation coefficient of the fits was greater than 0.95, in most cases it was better than 0.98.

Light calibration and calculation of rod activation. A scotopically corrected (for humans) photometer (International Light model IL1700, USA) with a luminance head was used to measure the average scotopic luminance (expressed in sc cd m^{-2}) of the stimulator's diffusing screen when the LEDs were activated with a 1 kHz train of current pulses each having a duration of 100 μs. (Keeping the duty cycle this low guaranteed that the power dissipation limit of the LEDs was not exceeded.) This enabled us to calculate the luminance of the stimulator during each light pulse assuming (as previously verified experimentally) that the luminance of the pulse was constant and independent of pulse duration. Each of the available luminance ranges was separately calibrated. Having made these measurements it was possible to calculate the luminance–time product for each of the single flash stimuli used (expressed in sc cd s m^{-2}). It should be noted that the spectral sensitivity of the mouse rods, determined using the ERG a-wave is very similar to the standard CIE scotopic spectral efficiency function for humans, justifying the use of a scotopically corrected photometer (Lyubarsky *et al.* 1999).

To calculate the activation level of the rods provided by these stimuli we proceeded as follows. First, we calculated the total light flux from the ganzfeld that could enter the eye through the pupil on the assumption that this is the light that was available to stimulate all the photoreceptors (neglecting at this stage various transmission and other losses). Since the essence of a ganzfeld is that the luminance of the stimulus is constant over the whole of the visual field (assumed to be hemispherical), the light entering the pupil is equal to the light flux emitted into a hemisphere by an area of the illuminated surface of the stimulator equal to that of the pupil. Thus, if the luminance of the stimulator is L (cd m^{-2}) and the pupil area is a (m^2), the light flux that could stimulate the retina is πaL lumens. Equivalently, if a flash stimulus has a luminance–time product of Lt (cd s m^{-2}), then πaLt lumens could be available to stimulate the retina. In fact it is often convenient to report stimulus strengths in terms of Trolands (the product of stimulus luminance in cd m^{-2} and pupil area measured in mm^2) rather than explicitly reporting both quantities. In this case, noting that aL is equal to $T \times 10^{-6}$, where T is the Troland value of the stimulus, a continuous stimulus of T td provides a light flux of $\pi T \times 10^{-6}$ lumens and a flash of Tt td s provides a luminous energy of $\pi Tt \times 10^{-6}$ lumen s.

To calculate the effect of a stimulus flash upon each rod in terms of the number of rhodopsin molecules that are photoisomerized the following steps are performed.

(a) Convert photometric measures to photon measures, noting that 1 sc lumen for rods is visually equivalent to 1.5×10^{15} photons s^{-1} of wavelength 507 nm (Wyszecki & Stiles, 1982). Thus a ganzfeld producing a 'retinal illuminance' of 1 td will provide $\pi \times 10^{-6}$ $1.5 \times 10^{15} = 4.7 \times 10^9$ photons s^{-1} and, equivalently, a flash of 1 td s will deliver 4.7×10^9 photons.

(b) Allow for losses resulting from reflection and absorption in the ocular media. It has commonly been assumed that about 70 % of incident light of wavelengths in the spectral region to which rods will respond reaches the retina. In the absence of specific information about the mouse eye we have adopted this minimum value for the transmission factor τ.

(c) Calculate the proportion of the whole retinal area occupied by the entrance aperture of a single rod. If the radius of the hemispheric eye is R and the radius of the circular entrance aperture of a rod is r, then the proportion of the total available photon flux entering a single rod is $r^2/2R^2$. Alternatively, for the area of the retina, A, the proportion of the total available photon flux entering a single rod is $\pi r^2/A$. We assume that the entrance aperture of the rods is equal to the cross-sectional area of the rod outer segments, which have a diameter of 1.4 μm in mice (Carter-Dawson & Lavail, 1979), and the average area of the retina in mice is 16.47 mm^2 (Jeon *et al.* 1998). Thus the proportion of the total available photon flux entering a single rod is:

$$\pi r^2/A = \mathrm{PA} = \pi \times (0.70)^2/(16.47 \times 10^6) = 9.35 \times 10^{-8}.$$

(d) Use an estimate of the outer segment axial optical density to determine what proportion of the light entering each rod is absorbed (PLR). Assuming a length for the rod outer segments of $l = 23.6$ μm (Carter-Dawson & Lavail, 1979) and a mean axial density per unit length δ of 0.0165 μm^{-1} (Lyubarsky & Pugh, 1996), $\mathrm{PLR} = 1 - 10^{-l\delta} = 1 - 10^{-(23.6 \times 0.0165)} \approx 0.59$.

(e) Allow for the quantum efficiency of photoisomerization. We adopted the conventional value of 0.67.

Taking all these factors into account, we calculate that 1 sc td s gives rise to:

$$\mathrm{Photons\ (td\ s)^{-1}} \times \tau \times \mathrm{PA} \times \mathrm{PLR} \times \mathrm{QE} =$$

$$4.7 \times 10^9 \times 0.7 \times 9.35 \times 10^{-8} \times 0.59 \times 0.67 \approx 121.6\ \mathrm{Rh^*}\ \text{per rod.}$$

This value is very similar to the value that we derived from calculations of Lyubarsky & Pugh (1996) and Pugh *et al.* (1998).

RESULTS

The scotopic ERG – amplitude–intensity relations

In previous studies of the dark-adapted ERG of the mouse a small positive-going b-wave, rather than a negative STR has generally been reported to be the 'threshold' ERG response to the weakest stimuli (e.g. Pugh *et al.* 1998; Toda *et al.* 1999). In the present study in order to determine whether a negative STR can be recorded in the fully dark-adapted mouse ERG, efforts were made to minimize noise.

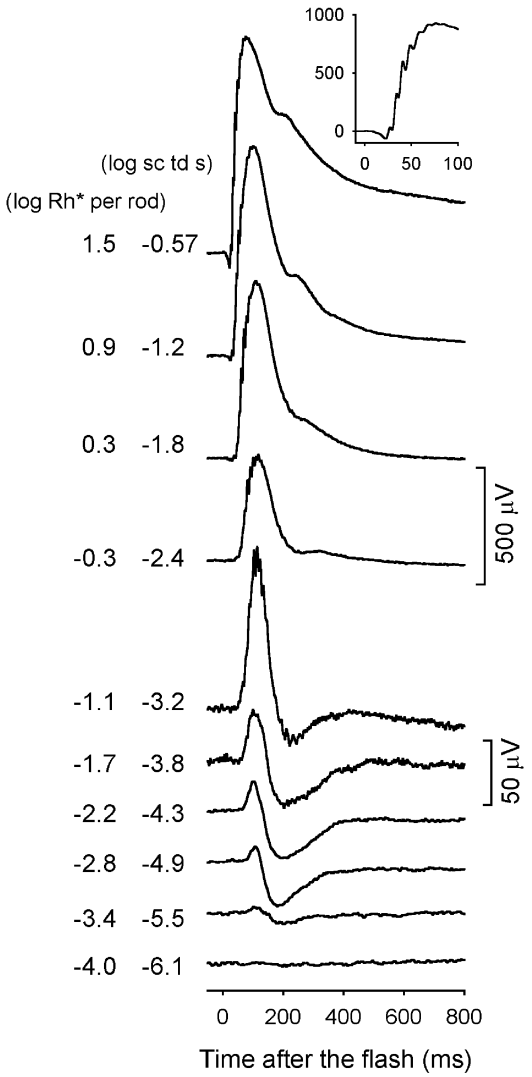

Figure 1. ERG responses to brief full-field flashes of increasing energy, from bottom to top, for one dark-adapted subject over the range of stimulus energies that generally were tested

Here and in subsequent figures, a brief flash occurred at time zero, and all flashes were < 5 ms in duration. The inset shows an ERG response (in μV) on an expanded time axis (ms) to a stimulus of −0.57 log sc td s to better illustrate the oscillatory potentials that were present when high energy flashes were used (subject MM180).

Noise due to respiratory and other movements and spontaneous oscillatory activity in the recording was reduced by stabilizing the animal's head, referencing the active ERG electrode to the contralateral eye to cancel common signals, and averaging responses to weak stimuli over many trials (40–60). Figure 1 shows typical mouse ERG responses, recorded under these conditions to brief flashes (< 5 ms) of increasing energy. A just-discernable response occurred for a flash energy of −5.5 log sc td s which gives rise, according to our calculations (see Methods), to about 1 photoisomerization per 2500 rods (−3.4 log Rh* per rod marked to the left of the trace). This small response contained a slow negative potential, reminiscent of the negative STR in other species that reached maximum amplitude around 200 ms after the flash. In addition, a small positive potential preceded the negative STR (nSTR). The positive potential reached its maximal amplitude around 110 ms after the flash.

Figure 1 shows that the amplitude of this sensitive negative potential increased with stimulus energy but stopped getting larger once the flash energy had been increased by a factor of 4 to −4.9 log sc td s. In contrast, the peak amplitude of the positive potential grew slowly over the initial 50-fold range of stimulus strengths (1.7 log units), increasing from 5 μV at −5.5 log sc td s, to 35 μV at −3.8 log sc td s (1 isomerization per 50 rods). In response to stronger stimuli, the increase in amplitude of the positive-going response accelerated, with the b-wave reaching an amplitude of nearly 1000 μV before fully saturating (note the change in amplitude calibration for the top four records in Fig. 1). Oscillatory potentials appeared on the top of the b-wave at −3.2 log sc td s, and on the leading edge of the response when the intensity reached −2.4 log sc td s. The a-wave emerged around −1.2 log sc td s.

To examine in more detail the most sensitive components of the dark-adapted ERG, Fig. 2 shows responses of another animal to a series of weak stimuli that successively doubled in energy over a more limited range. In this series the most sensitive response to a brief flash of −5.5 log sc td s showed mainly a small positive peak, but as in Fig. 1, this sensitive positive peak grew slowly over the initial 50-fold increase in stimulus energy, reaching 42 μV in response to a flash of −3.8 log sc td s. Although the negative potential was relatively small at −5.5 log sc td s, as in the previous figure, it was practically saturated in amplitude when the stimulus energy was increased to −4.9 log sc td s. The general relationship between the scotopic ERG and the stimulus strength illustrated in Figs 1 and 2 looked qualitatively similar across all animals.

In order to analyse, more quantitatively, the relationship of the ERG amplitude and stimulus energy, responses were measured at two fixed times after the brief stimulus flashes. The two times, marked by the vertical lines in Fig. 2, were: 110 ms after the flash, at the peak of the positive potential

in the ERG, and 200 ms after the flash, at the trough of the negative potential. As the ERG time course was quite similar from animal to animal (for example, compare Figs 1 and 2, and also control records in 5), these same times were used for all animals. ERG amplitudes measured at the two fixed times, 110 and 200 ms, and plotted *vs.* log flash energy are shown in Fig. 3*A* and *B*, respectively, for the 20 animals whose dark-adapted ERGs were measured over a large range of stimulus energies. In Fig. 4 results of four individual animals are illustrated. These two figures show that the amplitude–energy relation was quite similar across animals.

The positive amplitude of the ERG measured at 110 ms, i.e. the b-wave, grew to ~1000 μV in most cases and, due to the large range both of energies and amplitudes, was plotted in Figs 3*A* and 4 (left) on log–log axes. Measurements at 200 ms to assess the sensitive negative response, whose maximum amplitude was rarely larger than 50 μV, were plotted on log–linear axes. As observed for the traces in Figs 1 and 2, the plots in Figs 3*B* and 4 (right) show that the negative response grew from essentially zero up to saturation over less than one log unit range of energy (~4-fold). The plots also show that the response at 200 ms remained negative and near its saturated amplitude over another 20-fold increase in flash energy before it grew in a positive direction due to the growth of the b-wave.

Identifying and modelling ERG components

Although the amplitude–energy functions in Figs 3 and 4 show that the ERG is composed of both positive and

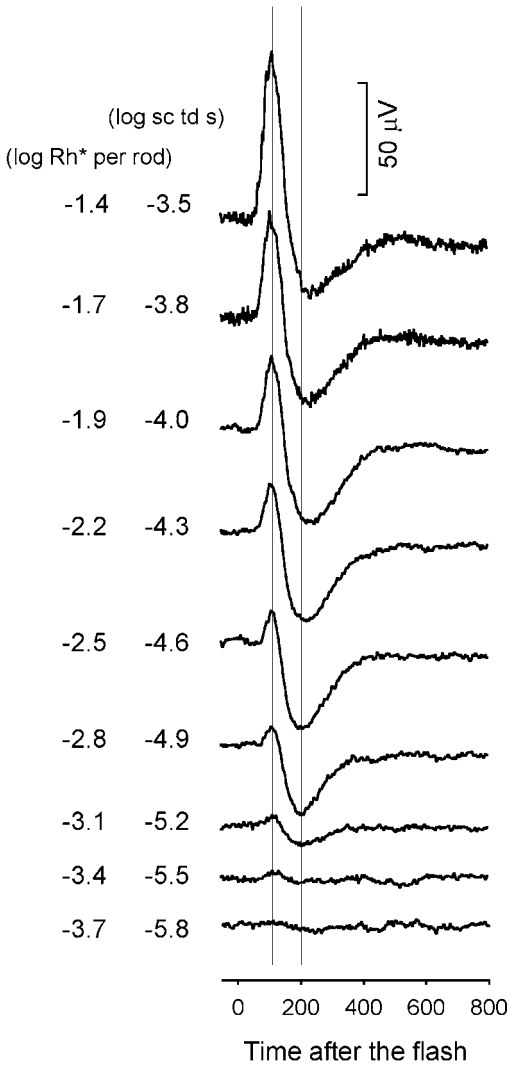

Figure 2. ERG responses to brief full-field flashes of increasing energy for one dark-adapted subject for the nine weakest stimuli that were tested

Stimulus energy doubled from bottom to top. The two vertical lines indicate where the positive peak and negative trough of the scotopic ERG occurred, 110 and 200 ms, after the flash, respectively (subject MM150).

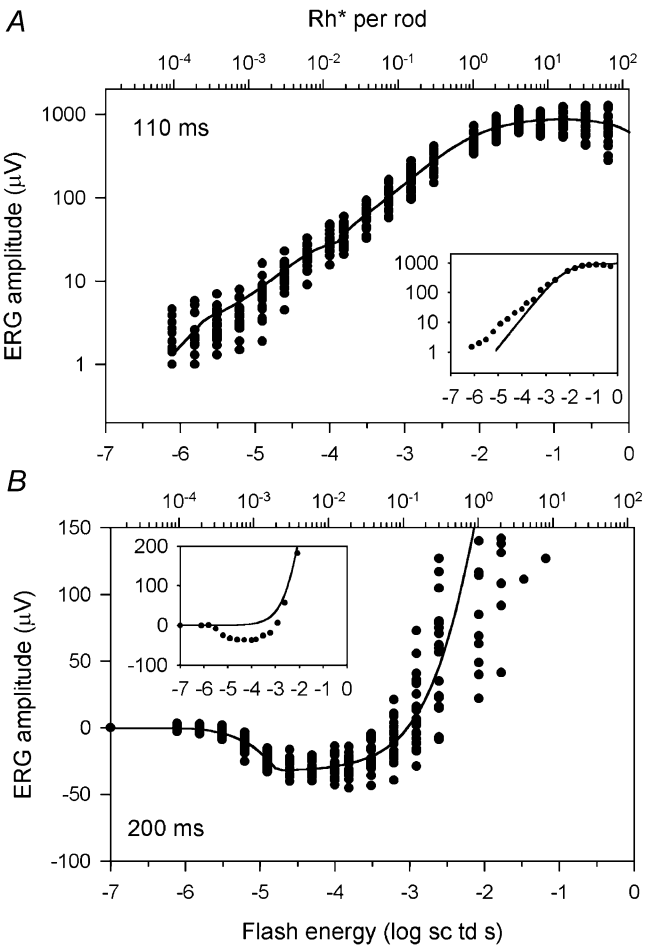

Figure 3. ERG amplitudes measured at fixed times after the stimulus for 20 subjects

A, ERG amplitudes measured at 110 ms after the flash plotted *vs.* stimulus energy (log sc td s), on the bottom axis and Rh* per rod on the top axis. The symbols represent the data and the continuous line represents the average five-component model fit to the data. The inset shows data from one subject (MM149) with a fitted hyperbolic function (eqn (1)) fitted to the saturation of the curve. *B*, ERG amplitudes measured at 200 ms after the flash. The format is as in *A*. The inset shows data from one subject (MM180), with a fitted hyperbolic function (data for high stimulus energies not shown).

negative components, simple inspection of the curves does not allow separation and characterization of those components. To facilitate identification of possible components, we endeavoured to fit plausible models of the underlying neuronal activity to the ERG amplitudes measured at fixed times. With regard to the dark-adapted b-wave, its amplitude–intensity relation has been described previously for the rat ERG as being linear for weak stimuli that produce sufficiently few photoisomerizations that the number of rods activated increased in proportion to stimulus strength (Cone, 1963). A linear amplitude intensity relation is reasonable, because the responses to quantal events by individual neurons in the mammalian retina from photoreceptors (Baylor *et al.* 1984) to retinal ganglion cells (Barlow *et al.* 1971) have been shown to increase initially in proportion to stimulus strength, before saturating. To describe the saturation of the b-wave amplitude–energy relation beyond its linear range, following Fulton & Rushton (1978), and many other investigators, we have used a hyperbolic function of the form:

$$V = V_{\max} I/(I + I_0), \quad (1)$$

where V is the ERG response amplitude, $V_{\max}$ is the maximum amplitude of the response, I_0 is the stimulus strength necessary to elicit a half-maximal response, and I is the strength of the stimulus flash that elicits the response (V).

To investigate the applicability of eqn (1) to the b-wave amplitude–energy relation in the present study, the equation was fitted (continuous lines, see Methods) to the saturation of the b-wave. Such fits are shown in the insets to Fig. 3*A* (110 ms) and *B* (200 ms) for data from individual animals (the whole function not shown in Fig. 3*B*). In both cases, and typical of all of our measurements, the responses to the weakest flashes clearly deviated from the linear portion of the function. For the measurements at 110 ms, the data fell above the fitted function at low stimulus energies, indicating greater sensitivity than predicted by the function. For the responses measured at 200 ms, the data fell below the fitted function at low energies, and in fact remained negative at all stimulus energies below about −2.5 log sc td s. For energies only slightly greater than this the data rapidly converged on the fitted function.

Previous work in the cat, using intraretinal recordings, or pharmacological blockade with GABA or glycine, or more recently NMDA (in rat as well as cat) has shown that the

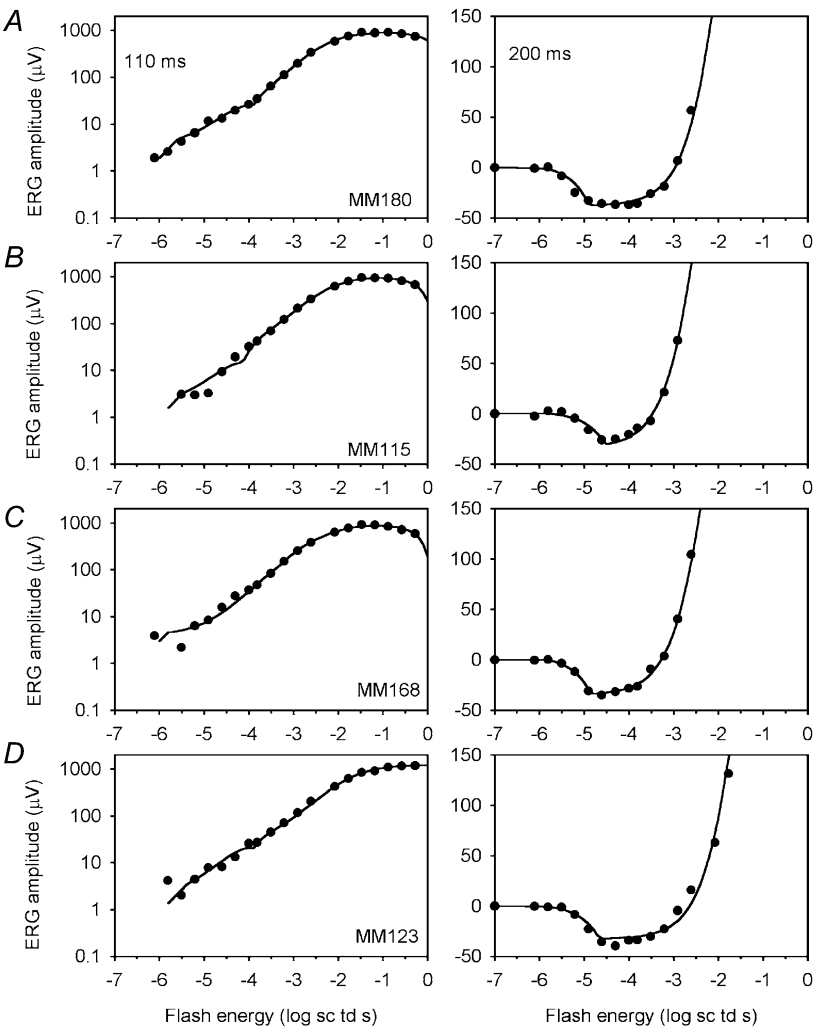

Figure 4. ERG amplitudes measured at fixed times after the stimulus for four different subjects

ERG amplitudes measured at 110 (left) and 200 ms (right) after the flash (●) are plotted *versus* stimulus energy (log sc td s). Each (left–right) pair of panels shows data from the same animal, as marked in the left-hand plot. The continuous line in each plot is the five-component model fitted to the data (see text). *A* and *B* show the best and worst fits, by eye, for data measured at 110 ms, and *C* and *D*, at 200 ms after the flash. Subject numbers are marked in the left-hand panels.

nSTR is generated more proximally in the retina than the b-wave, and it can be eliminated, without removing the b-wave (Sieving *et al.* 1986; Frishman & Steinberg, 1989*a,b*; Naarendorp & Sieving, 1991; Robson & Frishman, 1995). The b-wave that is pharmacologically isolated when more proximal retinal activity is suppressed is likely to reflect the activity of rod-driven bipolar cells, and is analogous to the positive process, PII, isolated in the dark-adapted cat ERG by Granit (1933). Pharmacologically isolated PII has been shown in cat (Robson & Frishman, 1995) and rat (Naarendorp *et al.* 2001) to rise linearly with stimulus energy at low energies, up to about 20 % of the response range, and then to saturate, following a hyperbolic function of the form of eqn (1). It is likely that PII reflects the activity specifically of rod bipolar cells (rather than rod-driven cone bipolar cells), at least at low light levels where cells are signalling single photoisomerizations in rods (Robson & Frishman, 1995).

In order to test the hypothesis that deviations from the hyperbolic function at low stimulus strengths in the mouse ERG reflect contributions from the proximal retina, GABA was injected intravitreally in three animals. In all three animals, as illustrated in Fig. 5 for one animal, GABA eliminated both the negative STR and the small sensitive positive potential. The remaining b-wave only became clearly visible at stimulus energy of about −4.3 log sc td s. GABA also removed oscillatory potentials, leaving smooth waveforms in response to all stimulus energies. In two of these animals, scotopic ERGs were recorded 2 weeks later, and were observed to have returned to the pre-GABA waveforms. Intravitreal injections of NMDA, used in previous studies in cat (Robson & Frishman, 1995) and rat (Naarendorp *et al.* 2001) to suppress inner retinal responses and to isolate PII, left a small residual negative STR in the mouse ERG ($n = 3$), and therefore the data are not shown.

Figure 6 shows plots of response amplitude at 110 and 200 ms after the flash as a function of stimulus energy for the control and post-GABA results shown in Fig. 5. The hyperbolic function (eqn (1), continuous curve) provides a good fit to the post-GABA data, showing that after GABA was injected positive-going responses to weak stimuli rose linearly with increasing energy before saturating.

The close approximation to linearity of the post-GABA ERG responses to weak stimuli was confirmed by scaling each response by the stimulus energy that elicited it to obtain a set of 'energy-scaled' versions of the responses. As demonstrated previously for PII in cat (Robson & Frishman, 1995) and rat (Naarendrop *et al.* 2001), after energy scaling, all responses generated by a single linear mechanism are of the same height and overall time course. The insets in the middle of Fig. 5 show overlaid responses to weak stimuli before and after GABA injection (left and right, respectively). After GABA the energy-scaled responses when superimposed

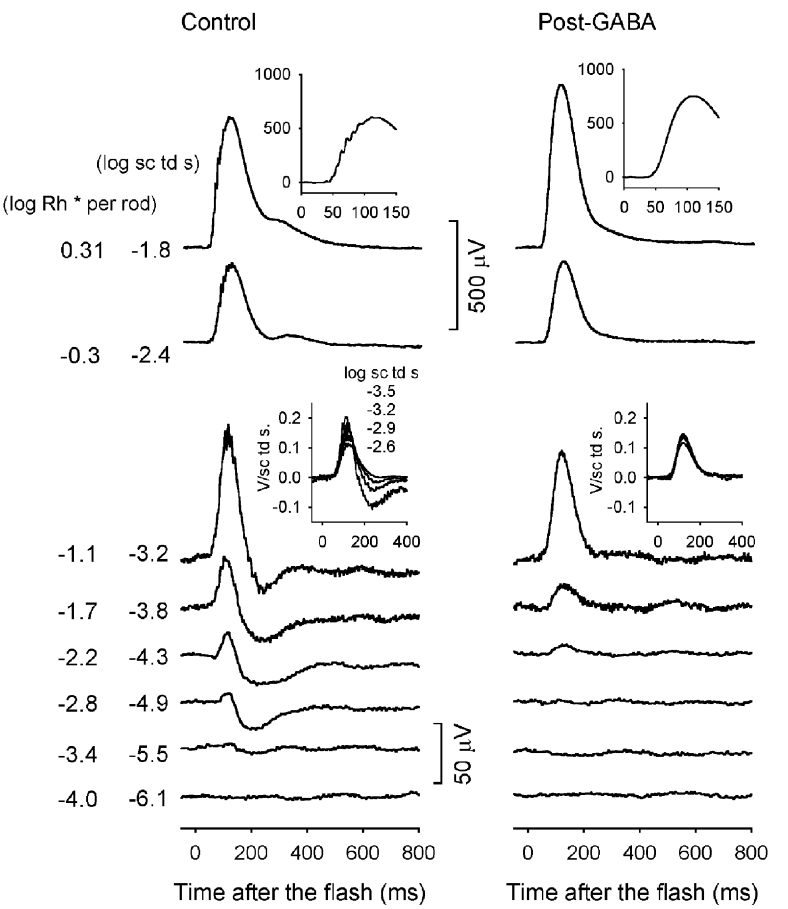

Figure 5. ERG responses to brief full-field flashes of increasing energy for one dark-adapted subject before (left) and after (right) injection of GABA

The insets in the middle of the figure show energy-scaled responses for the indicated energies. The insets at the top of the figure show responses (μV) to a high-energy flash on an expanded time axis (ms) to illustrate the effect of GABA on the oscillatory potentials (subject MM207).

matched well, showing that they had essentially identical waveforms. In contrast, before GABA, the responses did not superimpose as well, due to the presence of the nSTR and the saturating positive potentials.

The findings after GABA support the notion that the dark-adapted ERG of the mouse is composed of a combination of PII, presumably from rod bipolar cells, and more proximally generated inner-retinal components. GABA removed both positive and negative potentials, indicating the presence, in addition to the negative STR, of one or more sensitive positive components of proximal retinal origin. A positive STR, of similar sensitivity to the nSTR, has been described previously in the scotopic ERGs of humans, monkeys and cats (Frishman *et al.* 1996*a*,*b*), while a similar but less sensitive component has been described in rats (Naarendorp *et al.* 2001). In the mouse, however, the measurements made at 110 ms raise the possibility of there being more than one positive component more sensitive than PII in the ERG.

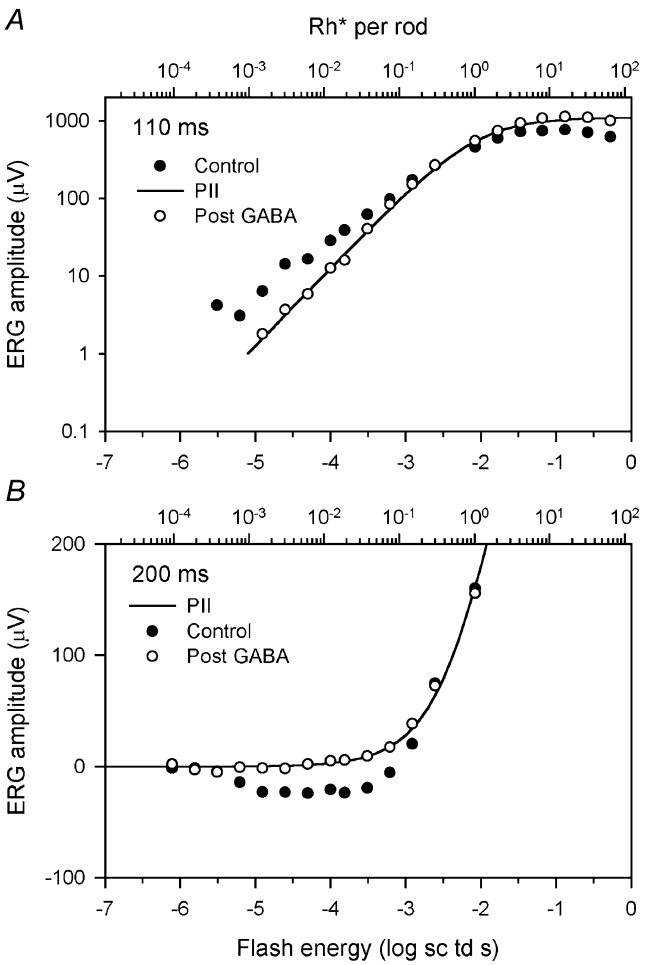

Figure 6. ERG amplitudes measured at 110 and 200 ms after the stimulus for the subject whose ERGs are illustrated Fig. 5 before (●) and after (○) injection of GABA

A, amplitudes measured at 110 ms with a hyperbolic function (eqn (1), line) fitted to the post-GABA data. *B*, ERG amplitudes measured at 200 ms with a hyperbolic function (eqn (1)) fitted to the post-GABA data for the same subject.

In Figs 3*A* (inset) and 6*A*, responses to stimuli between about −6 and −3.5 log sc td s rose more nearly in proportion to the square root of stimulus energy (i.e. with a slope that is closer to 0.5 than to 1 in the log–log plot). A log–log slope shallower than 1 is inconsistent with the response arising from a single class of neuron, if we assume, as argued above, that rod-driven responses of retinal neurons in mammalian retina all increase in proportion to stimulus strength (i.e. with a log–log slope of 1) before saturating. Thus, to model the responses measured at 110 ms, we appear to need, in addition to PII, two more sensitive positive components, each of which initially increases linearly with stimulus energy before saturating. Although both of these components could also contribute to the responses measured at 200 ms, the modelling described below suggests that the more sensitive of two components contributed relatively more at that time.

In addition to the positive components contributing to the ERG, a sensitive negative component, maximal 200 ms after a brief flash, also had to be included. Furthermore, in order to model responses to high-energy stimuli adequately it was necessary also to include the negative component from the photoreceptors, i.e. a component that at even higher stimulus energies would give rise to an a-wave. Thus, to explain the energy dependence of the amplitude of mouse scotopic ERG responses measured at fixed times after the stimulus flash, we adopted a model with a total of five components, each rising linearly with intensity before saturating. Three of these components – the nSTR, the pSTR and another positive response that we will call the positive scotopic response (pSR) to distinguish it from the pSTR – are assumed to come from proximal retina (amacrine and ganglion cells). The origins of the other two components, PII from rod-driven bipolar cells and PIII from rod photoreceptors, are better established.

Because the time course of none of the putative positive and negative components was known exactly, we initially assumed that all components contributed at both times for which amplitude measurements were made, independently adjusting the sensitivities at the two times to give the best fit. On the other hand, while the maximum amplitude of PII was also assumed to be different at the two times, the maximum amplitudes of the pSTR, the nSTR and the pSR were assumed to be the same.

In preliminary attempts to fit a model to the data, we examined how the form of the saturation function for each component affected the fit of the overall model to the data. We limited the form of saturation to three choices: hyperbolic, exponential or abrupt saturation (ramp). Hyperbolic and exponential functions have often been used to fit stimulus–response relations of distal retinal

neurons, whereas an abrupt saturation may be an appropriate description of spike trains (e.g. Sakmann & Creutzfeld, 1969). We found that only when applied to PII did the hyperbolic function of eqn (1) provide the best overall fit. In the case of both the negative and the positive STR, an abruptly saturating ramp described the data better. These ramp functions, as well as the other functions used in the overall fits are illustrated in Fig. 7 where they have been generated using average parameters from fits to all 20 animals illustrated in Fig. 3. The abruptly saturating ramp function rose linearly with increasing flash energy until it reached V_{max} at which value it then remained constant. For the ramp function, I_0 was the intensity at which the abrupt saturation occurred. For the pSR, an exponential function of the following form was found to be best:

$$V = V_{max}(1 - \exp(-I/I_0)). \quad (2)$$

The parameters are as defined for eqn (1), except for I_0 which was defined as the stimulus strength for which V was equal to $(1 - 1/e)V_{max}$. (I_0 is also the energy at which the response would reach V_{max} if it continued to rise at its initial rate). The photocurrent, PIII, was assumed to increase linearly with stimulus strength, but to be much less sensitive than the other components, having an amplitude of only 1 μV at −2 log sc td s. Hence effects of PIII on the ERG were significant only for the strongest stimuli. Because the amplitude of PIII was still quite small at the highest stimulus levels studied here, we simply assumed that it would increase in proportion to stimulus energy without saturation. Based upon the time course of the derived responses of mouse rods described by Hetling & Pepperberg (1999; their Fig. 5), the sensitivity of PIII (the slope of the linear rise of the response) at 200 ms after the flash was assumed to be half the sensitivity at 110 ms. Table 1 contains the average sensitivity of PIII and the other model components at the two analysis times. Average values of V_{max} for the four other components of the model are included.

The continuous lines in Fig. 4 show the fitted functions for four individual mice. The figure shows examples of the best and worst fits across animals. Panels *A* and *B* in Fig. 4 show the best and worst fits by eye for the data measured at

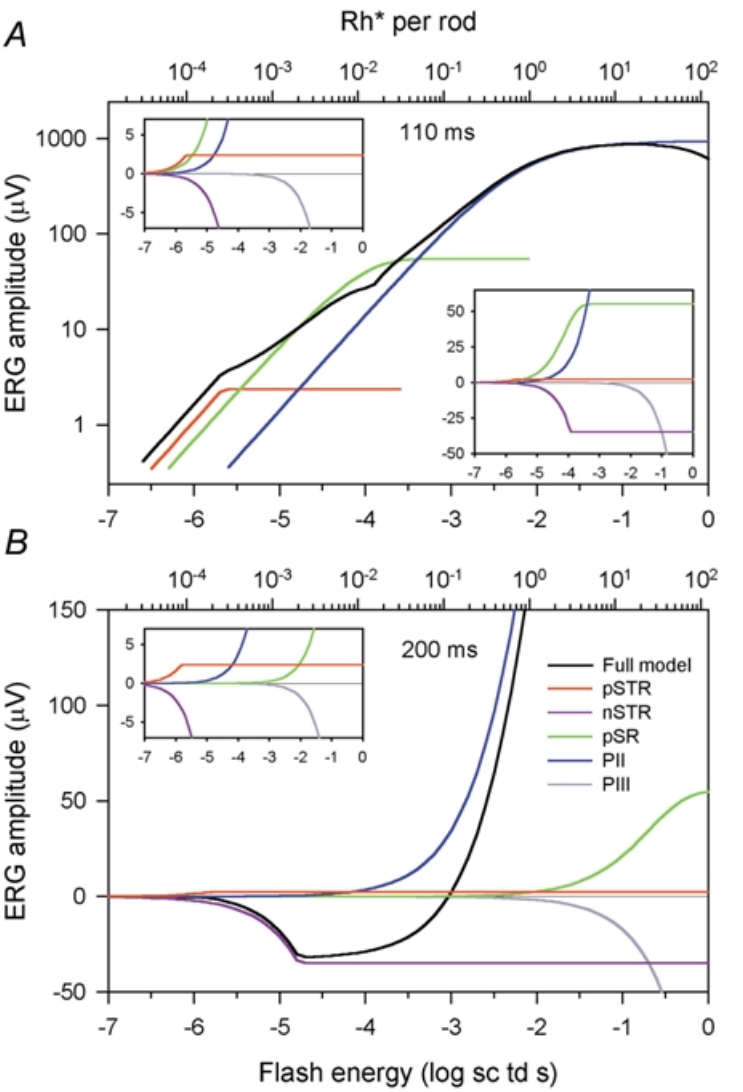

Figure 7. Model lines using average parameters from the 20 subjects illustrated in Fig. 3 for responses at 110 (*A*) and 200 ms (*B*) after the stimulus flash

For both times, the model included the five components: pSTR and nSTR (ramp with abrupt saturation), pSR (exponential saturation, eqn (2)), PII, (hyperbolic saturation, eqn (1)), and PIII (no saturation). The full model (black line) is decomposed into the five components (coloured lines). The insets have linear vertical axes (μV) so that the most sensitive model components of both polarities can be seen.

Table 1. Average parameters for model fits to the dark-adapted ERG of 20 mice

	Sensitivity (V (sc td s)$^{-1}$)		
	110 ms	200 ms	V_{max} (μV)
pSTR	1.1 ± 0.7	1.6 ± 0.8	2.4 ± 0.9
nSTR	0.2 ± 0.2	2.0 ± 0.9	35 ± 5.6
pSR	0.6 ± 0.3	(0.2 ± 0.1) × 10^{-3}	55 ± 18.4
PII	0.1 ± 0.05	0.03 ± 0.02	945 ± 211 (110 ms) 568 ± 124 (200 ms)
PIII	(0.4 ± 0.3) × 10^{-3}	(0.2 + 0.1) × 10^{-3}	—

110 ms (left), along with the results and fits for the results from the same animals measured at 200 ms (right). Panels *C* and *D* in Fig. 4 show the best and worst fits for the data at 200 ms (right), along with data from the same animals at 110 ms (left).

Fits deviated from the 110 ms data most at the lowest stimulus strengths, and for the 200 ms data most around the saturation of the nSTR. However, even in the worst cases fits were still quite good.

The continuous lines in Fig. 3 show the model based on average parameters for the 20 animals that are reported in Table 1. The component parts of the average model are illustrated in Fig. 7. The table contains sensitivity and V_{max} values for the various components rather than values for I_0 and V_{max}. Sensitivity (S) is defined as the amplitude of the response per unit stimulus energy for the range in which response amplitude is proportional to stimulus strength:

$$S = V/I = V_{max}/I_0. \quad (3)$$

The parameters are as defined previously for the various functions adopted for the different components.

Figure 7*A* and *B* and its insets show how the overall amplitude–energy functions are related to the components at each of the two times and how the very different shapes of these functions reflect differences in the relative sensitivities of the various components (see Table 1). At 200 ms (Fig. 7*B*) the amplitude–energy function at very low energies is essentially zero up to about −6 log sc td s because the only two components that are significant, the pSTR and the nSTR (see inset), have very nearly the same sensitivity and effectively cancel out. At higher energies

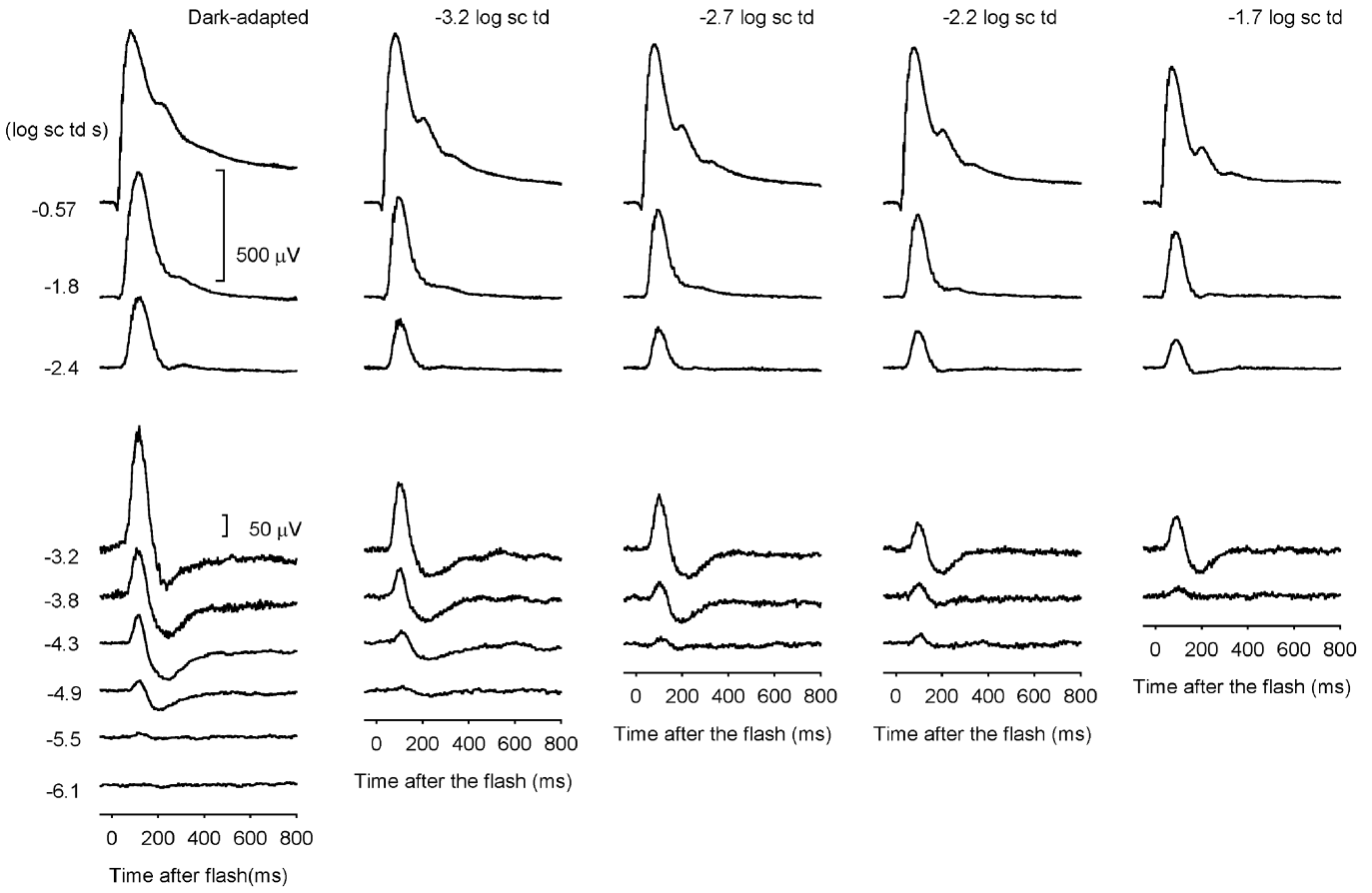

Figure 8. ERG responses under fully dark-adapted conditions in the presence of four steady backgrounds of increasing illumination from left to right in half log unit steps

Dark-adapted responses were recorded from one mouse (MM186) and responses to all backgrounds for a littermate (MM188) on the same day.

(from −6 to −4 log sc td s) the pSTR is saturated and the nSTR dominates the ERG. The ERG then remains negative until the less sensitive PII component overwhelms the saturated nSTR at −3 log sc td s and the ERG becomes positive. At 200 ms the pSR is so insensitive that it contributes very little to the ERG.

At 110 ms (Fig. 7*A*) the situation is different. As shown by the insets, the nSTR is less sensitive than it is at 200 ms (lower right), and it rises more slowly and is less sensitive than the pSTR (upper left). Perhaps more significant is that the rapidly rising pSR is the dominant contributor to the ERG at low energies. The net result is that the sum of all the positive components exceeds the nSTR at all energies. While this effectively obscures the contribution that the nSTR makes to the ERG, the nSTR does modify the shape of the overall amplitude–energy function whose log–log slope of less than one below about −3 log td s is primarily a reflection of the contributions of the pSR and pSTR.

Effects of light adaptation on the scotopic ERG

Previous studies of the light adaptation of ERGs and/or single-cell recordings in mammalian retina have shown that proximal retinal neurons are more sensitive to weak adapting backgrounds than are more distally located neurons (Green & Powers, 1982; Frishman & Sieving, 1995; Frishman *et al.* 1996*a*; Frishman & Robson, 1999; Naarendorp *et al.* 2001). To study the effects of background illumination on the mouse ERG and in particular to compare the effects on proximal retinal components with those on bipolar cells, ERGs were recorded under fully dark-adapted conditions and in the presence of various steady backgrounds.

ERGs from one animal recorded during the same session in the presence of four steady backgrounds of increasing illumination in 0.5 log unit steps are shown in Fig. 8. The responses recorded under fully dark-adapted conditions (left column) also were recorded in the same session, but from a littermate. The weakest background of −3.2 log sc td desensitized the responses so that the first discernable response occurred around −4.9 instead of −5.5 log sc td s or lower, in this and the previous Figures (1, 2 and 5) showing dark-adapted control data. Further increases in background illumination lead to greater desensitization so that, for a background of −1.7 log sc td, the response was first detectable for a flash energy of −3.8 log td s.

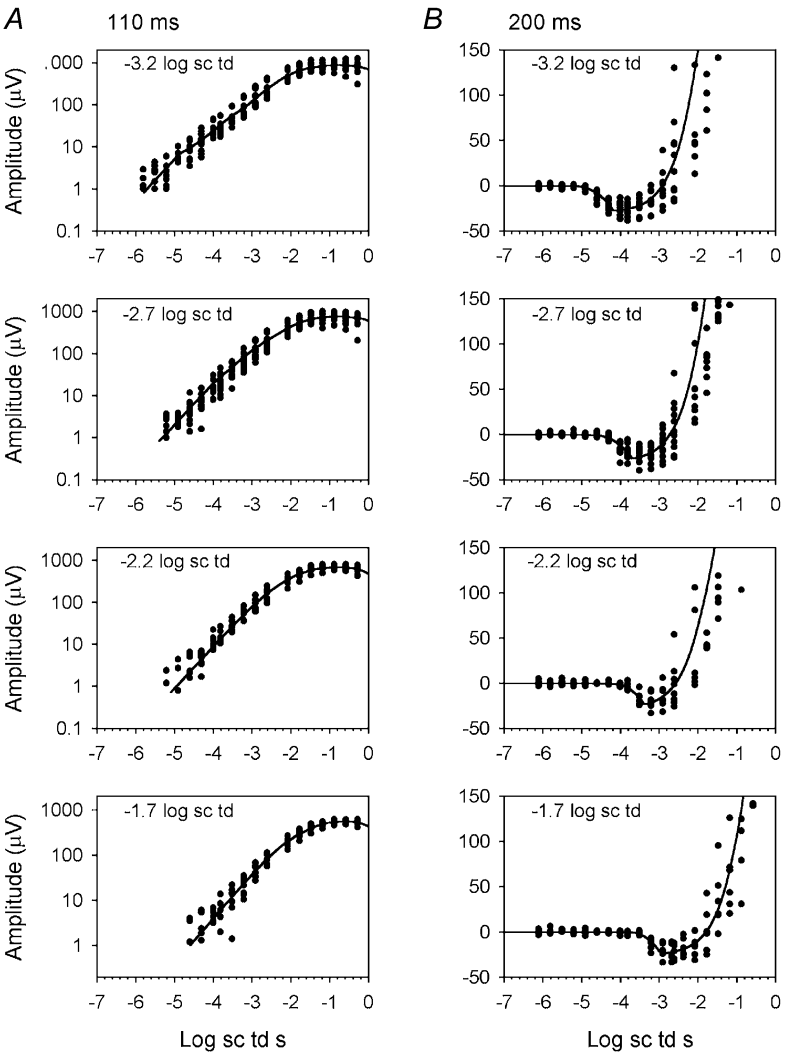

Figure 9. ERG amplitude at 110 (*A*) and 200 ms (*B*) for all subjects tested in the presence of steady backgrounds

● represent the data and the lines represent the model generated from average parameters for all of the subjects at each of the various backgrounds that were tested (10 subjects at −3.2, 11 subjects at −2.7, 8 subjects at −2.2 and 7 subjects at −1.7 log sc td).

Responses were measured at 110 and 200 ms after the stimulus for the four different background illuminations, and plotted *versus* stimulus energy. Figure 9 shows results at each background for groups of 7–11 animals (see figure legend). Most animals were studied under dark-adapted conditions and in the presence of at least two different backgrounds. Model curves were fitted to the responses using the same five-component model that we used for the dark-adapted data. The average model lines are shown in Fig. 9, and again in Fig. 10, in separate plots for the two analysis times. Figures 9 and 10 show that the negative-going responses at 200 ms and the responses to low-energy stimuli at 110 ms were more desensitized by increasing background illumination than the responses to higher-energy stimuli. While the general shape of the 200 ms curves was little changed by backgrounds, the slope of the lower portion of the 110 ms curves in Figs 9*A* and 10*A* grew steadily steeper, approaching a log–log slope of 1 as the background illumination was increased. For the highest two backgrounds, only a single hyperbolically saturating function (eqn (1); in combination with a small PIII) was needed to provide a good fit to the amplitude measurements made at 110 ms, suggesting that these backgrounds were strong enough to completely desensitize the proximal retinal components and leave just PII and PIII to form the ERG at this time. In contrast, for responses measured at 200 ms, although the negative-going responses were greatly desensitized, they were still present, reaching a similar maximum amplitude at each background level.

To illustrate the effect of the background on the sensitivity of each of the modelled components, Fig. 11 (lower plot) shows the relation between 1/sensitivity of each ERG component (except PIII) and background illumination. The sensitivity of the component was determined at the analysis time for which it was most sensitive under dark-adapted conditions (see Table 1). The data for each component were fitted with an equation that describes the Weber relation in which sensitivity declines in proportion to the increase in background illumination:

$$1/S = K(I + I_D), \quad (4)$$

where S is sensitivity, K is a constant, I is the background retinal illumination, and I_D is the level at which

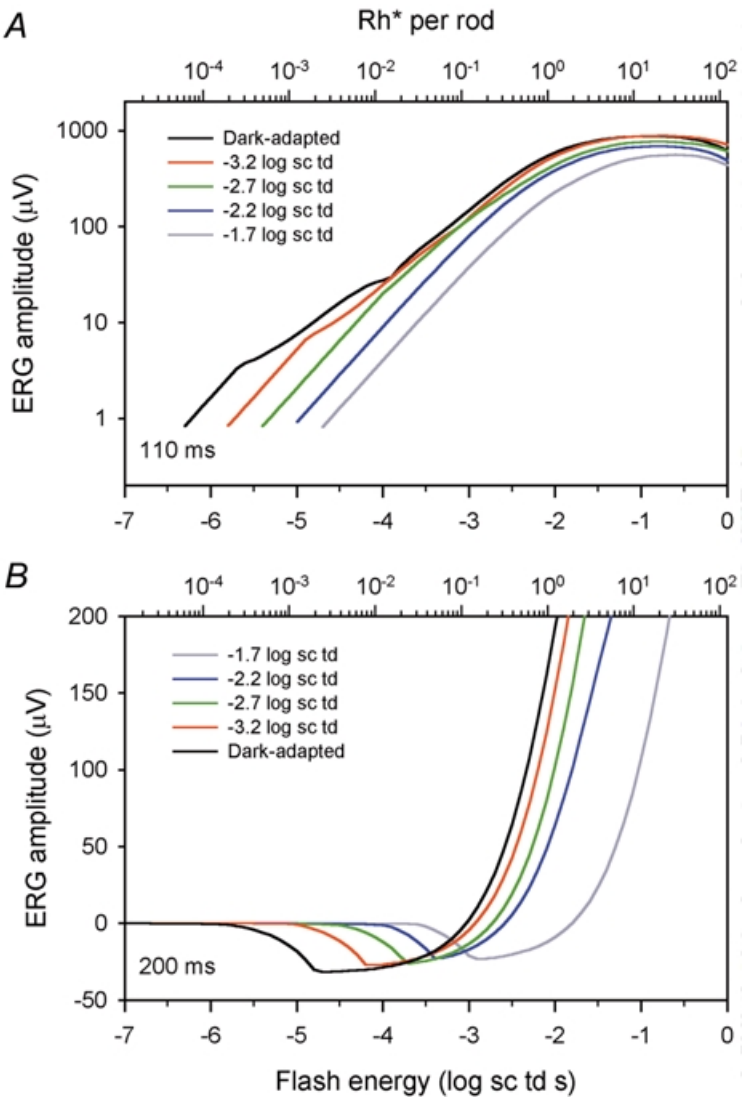

Figure 10. Effect of background illumination,model lines using average parameters

Model lines based on average parameters under dark-adapted conditions (black line, from Fig. 3) and in the presence of steady backgrounds (colours) from Fig. 9 at 110 (*A*) and 200 ms (*B*).

1/sensitivity has increased (i.e. sensitivity has decreased) by a factor of 2 (arrows in Fig. 11). I_D can also be interpreted as a 'dark light'. Dark light (Barlow, 1956, 1957) is a hypothetical internal signal, due at least in part to spontaneous isomerization in photoreceptors, that is equivalent to that produced by an external light giving a retinal illumination I_D. It sums with the signal generated by the actual background light to give the quantity that controls the sensitivity. The figure illustrates, as shown in Table 1, that the nSTR and pSTR were of similar sensitivity, and that the pSR was about 3 times less sensitive under fully dark-adapted conditions (bottom left). PII was more than 20 times less sensitive than the nSTR. (It should be realized that, in the context of the ERG, sensitivity differences cannot be simply interpreted as being of functional significance because they reflect not only the effectiveness of light in stimulating retinal cells, but also the effectiveness of the activity of those cells in generating an electrical signal that contributes to the ERG.)

The effect of steady backgrounds was similar for all three of the proximal retinal components (pSTR, nSTR and pSR) in the sense that the values for their dark light were indistinguishable, and the sensitivity of each was reduced to the same degree by any given background. This is better illustrated by the inset in the bottom panel where the sensitivity of the components has been normalized with respect to their dark-adapted value. The three proximal retinal components are superimposed, but PII, which was relatively unaffected by the weak backgrounds, showed an obvious increase in 1/sensitivity only for the strongest backgrounds.

The top panel of Fig. 11 shows the effect of background illumination on the modelled V_{max} for each component. While there was a slight reduction in the maximum amplitude of PII when the background was strong enough to reduce PII sensitivity, the maximum amplitude of the proximal retinal components was not greatly altered even by backgrounds that reduced the sensitivity by as much as 1.5–2 log units.

DISCUSSION

The present study has shown that the dark-adapted components of the mouse ERG that originate from proximal retina and are more sensitive than PII, are similar but not identical to those described for several other mammals. As observed previously in cats, monkeys, humans and rats, the dark-adapted ERG of the mouse

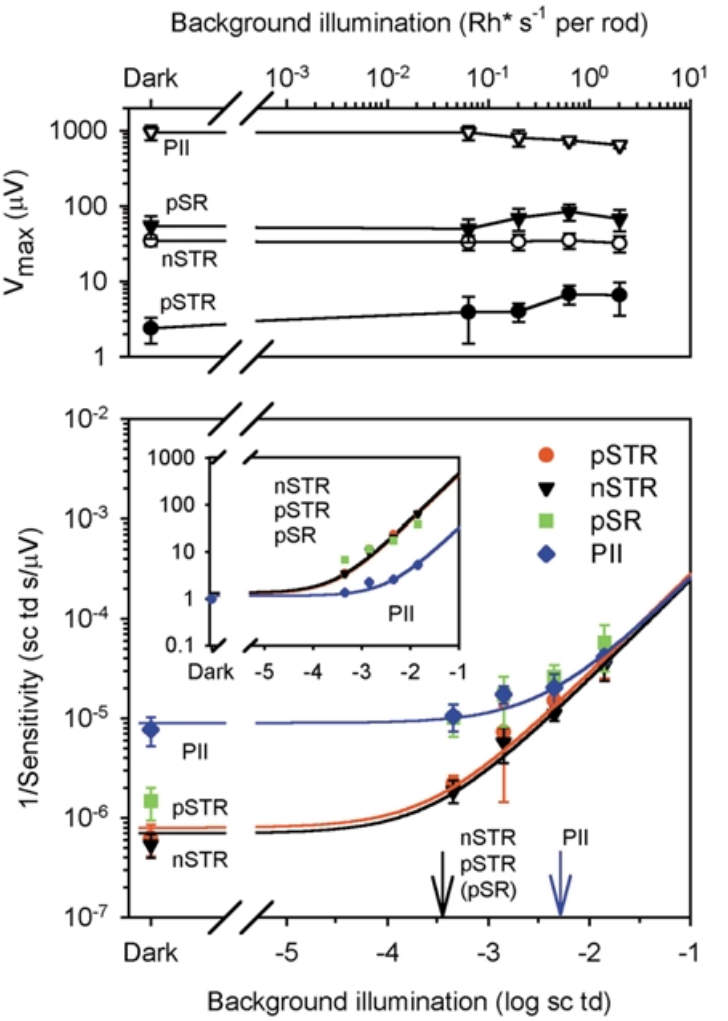

Figure 11. Effect of background illumination on model components

Lower panel, plot of 1/average sensitivity of four modelled components, nSTR at 200 ms, pSTR at 110 ms, pSR at 110 ms and PII at 110 ms. Sensitivity was calculated from the average model fits to the dark-adapted ERGs (Fig. 3 and Table 1), and the ERGs in the presence of steady backgrounds (Fig. 9). The lines represent a curve, $1/S = K(I + I_D)$ (eqn (4) in the text). The arrows mark the I_D (dark light) values for the three most sensitive model components, nSTR, pSTR and pSR on the left, and PII on the right. In the inset all components have been normalized for dark-adapted sensitivity. The upper panel shows the average V_{max} *versus* background illumination for the model components.

Table 2. Comparison of 'threshold' ERGs, VEPs, and behavioural threshold across studies in rodents

	log energy for −5 μV ERG	log energy for +5 μV ERG	nSTR V_{max} (μV)	PII V_{max} (μV)	log energy for a small VEP	Behavioural threshold
Current study (mouse)	−6.3 ± 0.2	−6.1 ± 0.2	34.8 ± 5.6	945 ± 211	—	—
Toda *et al.* (1999) (mouse)	—	−5.8 ± 0.2 *	—	765 **	—	—
Green *et al.* (1994) (rat)	—	−4.6 †	—	~ 525 ††	−6.4 ± 0.3 †††	—
Naarendorp *et al.* (2001) (rat)	−6.1 ‡	−4.8 ‡	21–24 ‡‡	628–887 ‡‡	—	−6.6 ± 0.3

All energies are stated in log scotopic cd s m^{-2}. * Value given in their paper (photopic), converted to scotopic by adding 0.2 log units; ** values taken from the legend to their Fig. 8. † Value estimated using equation and values provided throughout the paper; †† estimated from Fig. 2; ††† value given in paper (photopic cd m^{-2}), converted to scotopic by adding 0.3 log units, and to cd s m^{-2} (× 40/1000). ‡ Interpolated from their Fig. 1 using Rh* values and ERG amplitudes; ‡‡ taken from their Tables 1 and 2 using individual subject data.

includes a negative-going scotopic threshold response (nSTR) that can be separated from PII pharmacologically, and is more sensitive than PII to weak adapting backgrounds (Naarendorp *et al.* 1991; Frishman & Sieving, 1995; Frishman *et al.* 1996*a*; Naarendorp *et al.* 2001). Further, as observed in the other species, a small sensitive positive potential of proximal retinal origin is also present in the mouse ERG (Frishman *et al.* 1996*a,b*; Naarendorp *et al.* 2001). In other species, the sensitive positive potentials have been regarded as a single component. However, our model fits in mouse were better when two sensitive positive potentials were included: a very sensitive component (pSTR) that saturated when the response was quite small (~2.5 μV), and a slightly less sensitive component (pSR) that had a higher maximum response (~55 μV). These sensitive positive components contribute significantly to the mouse ERG. They dominate the b-wave responses to the weakest stimuli and over about a 100-fold range of increases in stimulus energy.

The failure in previous studies of the mouse dark-adapted ERG to consistently observe a negative STR is probably due mainly to the inherent noisiness in the *in vivo* recordings in mice caused in large part by respiratory movements and spontaneous oscillatory activity. Several steps were taken to improve the recording situation, including holding the head stationary, recording differentially between the two eyes and averaging over many trials when stimuli were weak and responses were small.

Sensitivity of the scotopic ERG

Table 2 shows results from this and other studies in rodents that measured the absolute sensitivity of the ERG, visually evoked potentials (VEPs) or behaviour, and in which stimulation and recording conditions were sufficiently similar that comparisons are feasible. The sensitivity of the mouse nSTR, judged by the luminance energy required to elicit a −5 μV response (Table 2, calculated from the model) was similar to that observed for the rat by Naarendorp *et al.* (2001). The maximum amplitude of the nSTR was small, about −35 μV, which was slightly larger than in the rat. V_{max} of the b-wave was much larger than V_{max} of the nSTR in both species (Table 2). However, changes in mouse vendor, strain or recording conditions (all of which were constant in the present study) can alter ERG amplitudes (S. M. Saszik, unpublished observations), making exact comparisons inappropriate. In general, though, in all species in which a nSTR has been observed, its maximum amplitude is about 3–4 % of that of the b-wave in the same recording session.

The sensitivity of the nSTR and the positive potential (b-wave) in our study was similar, whether based on average values from modelling (Table 1), or the luminance energy necessary to produce a 5 μV response (Table 2). The scotopic ERG (negative or positive) was 3–4 times more sensitive than the 'threshold' b-wave in recordings by Toda *et al.* (1999) from the same mouse strain, C57/BL6 (Table 2). Thus the most sensitive b-wave observed by Toda *et al.* occurred in response to stimuli that elicited a pSR in our study. In rat, even though the nSTR sensitivity was similar to that in mouse, the pSTR was less sensitive (Table 2), perhaps due to a species difference in its neuronal origin (see section below on retinal origins). For exact comparisons between our study and the others cited in Table 2, some caution is necessary, because we used blue LEDs whereas the other studies used white stimuli.

The rat's behavioural threshold was about 0.5 log units lower than the stimulus strength for a −5 μV nSTR in rat (Naarendorp *et al.* 2001), or mouse (Table 2). Similarly in humans, a −5 μV nSTR was observed for stimulus strengths that were 0.5–1.0 log units higher than the psychophysical threshold (Sieving & Nino, 1988; Frishman *et al.* 1996*a*). In contrast, visually evoked potential thresholds in rats, mice and humans were much closer to behavioural and psychophysical thresholds (Hayes & Balkema, 1993; Munoz Tedo *et al.* 1994; Green *et al.* 1994; Hansen & Fulton, 1995). However it is not clear to what extent further summation of quantal signals more

centrally in the visual pathway influences the VEP and behavioural/psychophysical thresholds.

Scotopic ERGs of cats, monkeys, humans, and now mice, have now been measured in our laboratory using the same (blue LEDs), or for humans, similar (green LEDs), stimuli. We have found, as previously reported by Sieving & Wakabayashi (1991) for cats, monkeys and humans (using an 80 ms stimulus), that the external luminance energy (sc cd s m^{-2}) of the brief stimulus that elicits 'threshold' ERG responses is quite similar across species. However, humans required more than 6 times greater stimulus energy to produce a −5 μV ERG than the other species (Frishman *et al.* 1996*a*). This possible difference between humans and other species can be clarified by using exactly the same stimuli across species.

Although we found that the external luminance required for a small ERG response was similar in mice, monkeys and cats, about −6.3 log sc cd s m^2 for monkeys and mice, and about 0.3 log units less for cats, the retinal illuminance (sc td s at the cornea, defined as luminance times pupil area) increased as eye size, and the related dilated pupil area increased (Table 3). However, when we converted the illuminance to photoisomerizations per rod (Rh*), the necessary quantal catch for a small criterion response become more similar again. This occurred primarily because the size of rod photoreceptors is similar among species despite differences in eye size, leading, as shown in Table 3, to greater Rh* per rod per sc td s for small eyes. The required quantal catch for a small response for mice, monkeys and cats (Table 3) was lower than that observed for rats, which was 1 in 433 rods (Naarendorp *et al.* 2001).

Table 3. Comparison of sensitivity in three different species, using the same stimulus conditions

	Mouse	Monkey	Cat
log sc cd m^{-2} s	−6.3	−6.3	−6.6
Pupil area (mm^2)	7.1	63.5	133
log sc td s	−5.5	−4.6	−4.5
Rh* per sc td s	122	12.5	5
log Rh* per rod	−3.4	−3.5	−3.8
Rods per Rh*	2653	2886	6889

Modelled components and their retinal origins

Modelling allowed us to estimate the sensitivity and amplitude of contributions from ERG components that could not easily be separated by inspection. A similar model, having an nSTR, but including only one positive component more sensitive than PII, was used previously to fit data from cats and humans (Frishman *et al.* 1996*a*; Frishman & Robson, 1999). How confident can we be that the present five-component model provides an accurate description of the mouse ERG? The fits themselves were very good (see Results), and were improved at both analysis times, by the addition of a second sensitive positive potential. However, to answer the question, it is important to examine the assumptions in the modelling. The fundamental assumption that retinal processing of quantal events is linear is well supported by previous work in single cells in mammalian retina (e.g. Barlow *et al.* 1971; Baylor *et al.* 1984; Berntson & Taylor, 2000; Euler & Masland, 2000). Although supralinear behaviour has recently been reported for mouse rod bipolar cell responses in a slice preparation (Field & Rieke, 2002), it was observed for stimuli that exceeded 1 Rh* per rod and therefore would saturate PII in the present study. The assumption that a photoreceptor PIII was present in responses to high stimulus energies at both analysis times is supported by studies in mice and other species using pharmacological blockers, paired flash techniques, and genetic manipulations (e.g. Robson & Frishman, 1995, 1998; Hetling & Pepperberg, 1999; Kang-Derwent *et al.* 2002).

The identification of the scotopic PII component of the ERG with rod bipolar cells, at least for responses to weak stimuli, was suggested in previous studies in cat and rat where the component was pharmacologically isolated using intravitreal NMDA, kainate/AMPA blockade, or GABA (Robson & Frishman, 1995; Green & Kapousta, 1999; Naarendorp *et al.* 2001). The mouse, like these other species, has only one class of bipolar cells that carries exclusively rod signals. However, rod signals travelling in cone bipolar cells might also contribute to PII, particularly as light levels are increased (e.g. Smith *et al.* 1986). Those signals could enter via gap junctions (connexin 36) between rods and cones, or via gap junctions between AII amacrine cells and On cone bipolar cells (Guldenagel *et al.* 2001). PII also included a small amount of cone signals in response to strong stimuli. We measured the cone contribution by recording responses to test stimuli 300–3000 ms after suppressing rod signals (Lyubarsky *et al.* 1999) and established that their contribution was < 10 % of the saturated b-wave. Therefore, our modelling was minimally affected by cone signals.

One can ask whether intravitreal GABA altered the responses that rod bipolar cells contributed to PII. Despite the presence of GABA receptors on rod bipolar terminals and receptors and transporters elsewhere in the inner plexiform layer (IPL), as well as in the outer plexiform layer (OPL), of the mouse retina (Haverkamp & Wässle, 2000; McCall *et al.* 2002; Cueva *et al.* 2002), GABA-isolated PII responses showed sensitivity and a linear stimulus–response relation that closely approximated the linear model of PII fit to control data (Fig. 6). Single-cell experiments would be needed to determine why flooding the retina with GABA, thereby eliminating spatial and stimulus-related temporal variations in its local concentration, does not appear to alter the fundamental response characteristics of the cells that generate PII. One might speculate that the $GABA_C$ receptors that are

predominant on rod bipolar cells (e.g. McCall *et al.* 2002), as well as other GABA receptors, were desensitized and the GABA transporters were overwhelmed by the injected GABA, but these issues cannot be resolved in ERG studies.

Recent work in mouse retina indicates the existence of another pathway for rod signals in which 20 % of the rods synapse directly on Off cone bipolar cells (Tsukomoto *et al.* 2001). If this pathway produces ERG signals of proximal retinal origin, then they should persist in the presence of L-2-amino-4-phosphonobutyric acid (APB), a glutamate analogue that blocks transmission from photoreceptors to On bipolar cells. However, in preliminary studies, APB was found to eliminate all postreceptoral responses in the dark-adapted ERG of the mouse (S. M. Saszik & L. J. Frishman, unpublished observations).

The results using GABA in the mouse support the proposal that the pSTR, the nSTR, and the pSR originate from the rod circuits proximal to the bipolar cells, as do the sensitive components in other species in which their origins have been studied more extensively (e.g. in cat by Frishman & Steinberg, 1989*a,b*; Naarendorp *et al.* 1991). However, we do not know the exact cellular origins of these components. Aside from the various classes of ganglion cells, the primary candidate amacrine cells, as for the other sensitive components, would be the AII and A17 cells in the rod circuit. Responses of all of these cells would be GABA sensitive (e.g. Bloomfield & Xin, 2000; Menger & Wässle, 2000). In considering their origins, it is important to realize that each component does not necessarily arise from a single class of neurons, or selectively either from spiking or non-spiking activity of amacrine and ganglion cells. In this sense our modelling indicates the minimum number of components that might be present.

Although, we do not know the exact cellular origins of the sensitive ERG components, we have some insights from other studies. For instance, whether the nSTR is dominated by amacrine or ganglion cell responses appears to be species dependent. In macaque monkeys it is likely that the nSTR arises predominantly from ganglion cells; it is absent from eyes in which ganglion cells were eliminated as a consequence of laser-induced ocular hypertension (Frishman *et al.* 1996*b*). In contrast, in cats and humans the response may be more amacrine-cell related; following degeneration of ganglion cells due to optic nerve section or atrophy, the nSTR was not eliminated (Sieving, 1991). Experiments with intravitreal tetrodotoxin (TTX) to block Na^+-dependent action potentials in amacrine and ganglion cells (where they most commonly occur in the retina) showed that the monkey nSTR is driven by spiking activity (Ahmed *et al.* 1999), whereas in cats it is only partly driven by such activity (Frishman & Robson, 1996).

The cat nSTR has been shown to be mediated by K^+ 'spatial buffer' currents that flow from proximal to distal retina in retinal glia, i.e. Müller cells (Frishman & Steinberg, 1989*a,b*). Intraretinal recordings with ion-selective electrodes indicated that these currents occur as a result of elevated $[K^+]_o$ in proximal retina following depolarization of the local neurons in response to light onset, but not light offset (Frishman & Steinberg, 1989*b*), suggesting that the nSTR originates from On pathway neurons. Radial astrocytes in the optic nerve head may produce K^+ currents as a consequence of ganglion cell depolarization that also contribute to the ERG, as suggested for the photopic negative response of the macaque ERG (Viswanathan *et al.* 1999).

A characteristic of glially mediated ERG responses is their slow time course. In cats the nSTR peaks > 50 ms later than the scotopic b-wave. In mice and monkeys the difference can be even greater, suggesting glial mediation in these species as well. Glial mediation of the nSTR may explain the similarity of its time course and maximum amplitude across species regardless of the particular local neurons that are affecting proximal retinal $[K^+]_o$. The relative contribution from different neuronal classes might depend upon the numbers of cells in sensitivity to adapting backgrounds

Based on the differential sensitivity of distal and proximal retinal potentials to background illumination, it has been suggested that the adaptation in the mammalian retina occurs in stages (Green & Powers, 1982; Frishman & Sieving, 1985; Frishman & Robson, 1999). The present study supports this proposal; the components thought to be generated in retina proximal to the PII generator all were desensitized by backgrounds at least 20 times weaker than the background that desensitized PII. In the rat, the difference was greater, with the background that reduced nSTR sensitivity by a factor of 2 being 100 times weaker than the one that desensitized PII, and previous similar work in cats, monkeys and humans yielded differences at least as great (Frishman & Sieving, 1995). Convergence of rod signals could be one mechanism for adaptation in proximal retina (e.g. Frishman *et al.* 1996*a*), although other mechanisms might also be involved (Naarendorp *et al.* 2001).

Another interesting outcome of the adaptation experiments was that V_{max} of the mouse STR did not change substantially as background illumination was increased, whereas PII V_{max} began to decline. This suggests mechanisms to adjust the sensitivity of proximal retinal neurons that maintain the neurons' full operating range, as demonstrated by Sakmann & Creutzfeld (1969) for cat ganglion cells. Further studies should provide insights about these mechanisms.

The explosion of research involving genetically altered mice as a model (e.g. see Malakoff, 2000) reflects the importance of understanding the function of normal animals. This study has presented an in-depth look at the

dark-adapted ERG of the mouse. The results show that the scotopic ERG response to weak stimuli in mouse is similar to that in other mammalian species, including humans. The current work establishes the utility of the mouse ERG for studying rod-driven retinal function that originates from circuits proximal to the bipolar cell, in addition to its use in studying processing of rod signals that occurs more distally in the retina.

REFERENCES

Ahmed, J., Frishman, L. J. & Robson, J. G. (1999). Pharmacological removal of positive and negative STRs is required to isolate bipolar-cell responses in the macaque scotopic electroretinogram. *Investigative Ophthalmology and Visual Science,* suppl. 40, S15.

Barlow, H. B. (1956). Retinal noise and absolute threshold. *Journal of the Optical Society of America,* **46**, 634–639.

Barlow, H. B. (1957). Increment thresholds at low intensities considered as signal/noise discriminations. *Journal of Physiology* **136**, 469–488.

Barlow, H. B., Levick, W. R. & Yoon, M. (1971). Responses to single quanta of light in retinal ganglion cells of the cat. *Vision Research* **11**, suppl. 3, 87–102.

Baylor, D. A., Nunn, B. J. & Schnapf, J. L. (1984). The photocurrent, noise and spectral sensitivity of rods of the monkey *Macaca Fascicularis*. *Journal of Physiology* **357**, 575–607.

Berntson, A. & Taylor, W. R. (2000). Response characteristics and receptive field widths of on-bipolar cells in the mouse retina. *Journal of Physiology* **524**, 879–889.

Bloomfield, S. A. & Xin, D. (2000). Surround inhibition of mammalian AII amacrine cells is generated in the proximal retina. *Journal of Physiology* **523**, 771–783.

Bush, R. & Reme, C. E. (1992). Chronic lithium treatment induces reversible and irreversible changes in the rat ERG *in vivo*. *Clinical Vision Sciences* **5**, 393–401.

Carter-Dawson, L. D. & Lavail, M. M. (1979). Rods and cones in the mouse retina. Structural analysis using light and electron microscopy. *Journal of Comparative Neurology* **188**, 245–262.

Cone, R. A. (1963). Quantum relations of the rat electroretinogram. *Journal of General Physiology* **46**, 1267–1286.

Cueva, J. G., Haverkamp, S., Reimer, R. J., Edwards, R., Wässle, H. & Brecha, N. C. (2002). Vesicular gamma-aminobutyric acid transporter expression in amacrine and horizontal cells. *Journal of Comparative Neurology* **445**, 227–237.

Dawson, W. W., Trick, G. L. & Litzkow, C. A. (1979). Improved electrode for electroretinography. *Investigative Ophthalmology and Visual Science* **18**, 988–991.

Euler, T. & Masland, R. H. (2000). Light-evoked responses of bipolar cells in a mammalian retina. *Journal of Neurophysiology* **83**, 1817–1829.

Field, G. & Rieke, F. (2002). Nonlinear signal transfer from mouse rods to bipolar cells and implications for visual sensitivity. *Neuron* **30**, 773–785.

Frishman, L. J., Reddy, M. G. & Robson, J. G. (1996*a*). Effects of background light on the human dark-adapted ERG and psychophysical threshold. *Journal of the Optical Society of America A* **13**, 601–612.

Frishman, L. J. & Robson, J. G. (1999). Inner retinal signal processing: adaptation to environmental light. In *Adaptive Mechanisms in the Ecology of Vision*, ed. Archer, S. N., Djamgoz, M. B. A., Loew, E. R., Partridge, J. C. & Vallerga, S., pp. 383–412. Chapman and Hall Ltd, Kluver, London.

Frishman, L. J., Shen, F. F., Du, L., Robson, J. G., Harwerth, R. S., Smith, E. L. III, Carter-Dawson, L. & Crawford, M. L. (1996*b*). The scotopic electroretinogram of macaque after retinal ganglion cell loss from experimental glaucoma. *Investigative Ophthalmology and Visual Science* **37**, 125–141.

Frishman, L. J. & Sieving, P. A. (1995). Evidence for two sites of adaptation affecting the dark-adapted ERG of cats and primates. *Vision Research* **35**, 435–442.

Frishman, L. J. & Steinberg, R. H. (1989*a*). Intraretinal analysis of the threshold dark-adapted ERG of cat retina. *Journal of Neurophysiology* **61**, 1221–1232.

Frishman, L. J. & Steinberg, R. H. (1989*b*). Light-evoked increases in $[K^+]_o$ in proximal portion of the dark-adapted cat retina. *Journal of Neurophysiology* **61**, 1233–1243.

Fulton, A. B. & Rushton, W. A. H. (1978). The human rod ERG: correlation with psychophysical responses in light and dark adaptation. *Vision Research* **18**, 793–800.

Green, D. G., Herreros De Tejada, P. & Glover, M. J. (1994). Electrophysiological estimates of visual sensitivity in albino and pigmented mice. *Visual Neuroscience* **11**, 919–925.

Green, D. G. & Kapousta-Bruneau, N. V. (1999). A dissection of the electroretinogram from the isolated rat retina with microelectrodes and drugs. *Visual Neuroscience* **16**, 727–741.

Green, D. G. & Powers, M. K. (1982). Mechanisms of light adaptation in rat retina. *Vision Research* **22**, 209–216.

Granit, R. (1933). The components of the retinal action potential in mammals and their relation to the discharge in the optic nerve. *Journal of Physiology* **77**, 207–239.

Guldenagel, M., Ammermuller, J., Feigenspan, A., Teubner, B., Degen, J., Sohl, G., Willecke, K. & Weiler, R. (2001). Visual transmission deficits in mice with targeted disruption of the gap junction gene connexin36. *Journal of Neuroscience* **21**, 6036–6044.

Hansen, R. M. & Fulton, A. B. (1995). The VEP thresholds for full-field stimuli in dark-adapted infants. *Visual Neuroscience* **12**, 223–228.

Haverkamp, S. & Wässle, H. (2000). Immunocytochemical analysis of the mouse retina. *Journal of Comparative Neurology* **424**, 1–23.

Hayes, J. M. & Balkema, G. W. (1993). Elevated dark-adapted thresholds in hypopigmented mice measured with a water-maze screening apparatus. *Behavior Genetics* **23**, 395–403.

Hetling, J. R. & Pepperberg, D. R. (1999). Sensitivity and kinetics of mouse rod flash responses determined *in vivo* from paired-flash electroretinograms. *Journal of Physiology* **516**, 593–609.

Jeon, C. J., Strettoi, E. & Masland, R. H. (1998). The major cell populations of the mouse retina. *Journal of Neuroscience* **18**, 8936–8946.

Kang-Derwent, J. J., Saszik, S. M., Pardue, M. T., Frishman, L. J. & Pepperberg, D. R. (2002). Response properties of rod photoreceptors in nob mice determined by paired-flash electroretinography. *Investigative Ophthalmology and Visual Science*, suppl. 43, 1838.

Lyubarsky, A. L., Falsini, B., Pennesi, M. E., Valentini, P. & Pugh, E. N. Jr (1999). UV- and midwave-sensitive cone-driven retinal responses of the mouse: a possible phenotype for coexpression of cone photopigments. *Journal of Neuroscience* **19**, 442–455.

Lyubarsky, A. L. & Pugh, E. N. Jr (1996). Recovery phase of the murine rod photoresponse reconstructed from electroretinographic recordings. *Journal of Neuroscience* **16**, 563–571.

McCall, M. A., Lukasiewicz, P. D., Gregg, R. G. & Peachey, N. S. (2002). Elimination of the rho1 subunit abolishes GABA(C). receptor expression and alters visual processing in the mouse retina. *Journal of Neuroscience* **22**, 4163–4174.

Malakoff, D. (2000). The rise of the mouse, biomedicine's model mammal. *Science* **288**, 248–253.

Menger, N. & Wässle, H. (2000). Morphological and physiological properties of the A17 amacrine cell of the rat retina. *Visual Neuroscience* **17**, 769–780.

Miller, R. F. & Dowling, J. E. (1970). Intracellular responses of Müller (glial) cells of mudpuppy retina: their relation to the b-wave of the electroretinogram. *Journal of Neurophysiology* **33**, 323–341.

Munoz Tedo, C., Herreros De Tejada, P. & Green, D. G. (1994). Behavioral estimates of absolute threshold in rat. *Visual Neuroscience* **11**, 1077–1082.

Naarendorp, F., Sato, Y., Cajdric, A. & Hubbard, N. P. (2001). Absolute and relative sensitivity of the scotopic system of rat: electroretinography and behavior. *Visual Neuroscience* **18**, 641–656.

Naarendorp, F. & Sieving, P. A. (1991). The scotopic threshold response of the cat ERG is suppressed selectively by GABA and glycine. *Vision Research* **31**, 1–15.

Penn, R. D. & Hagins, W. A. (1969). Signal transmission along retinal rods and the origin of the electroretinographic a-wave. *Nature* **223**, 201–204.

Pugh, E. N. Jr, Falsini, B. & Lyurbarsky, A. (1998). The origin of the major rod- and cone-driven components of the rodent electroretinogram and the effects of age and light-rearing history on the magnitude of these components. In *Photostasis and Related Phenomena,* pp. 93–128. Plenum Press, New York.

Robson, J. G. & Frishman, L. J. (1995). Response linearity and kinetics of the cat retina: the bipolar cell component of the dark-adapted electroretinogram. *Visual Neuroscience* **12**, 837–850.

Robson, J. G. & Frishman, L. J. (1999). Dissecting the dark-adapted electroretinogram. *Documenta Ophthalmologica* **95**, 187–215.

Sakmann, B. & Creutzfeld, O. J. (1969). Scotopic and mesopic light adaptation in the cat's retina. *Pflüger's Archiv* **313**, 168–185.

Saszik, S. M., Wu, J., Robson, J. G. & Frishman, L. J. (2001). The scotopic threshold response of the dark-adapted ERG of the mouse. *Investigative Ophthalmology and Visual Science* **42**, suppl.

Shiells, R. A. & Falk, G. (1999). Contribution of rod, on-bipolar, and horizontal cell light responses to the ERG of dogfish retina. *Visual Neuroscience* **16**, 503–511.

Sieving, P. A. (1991). Retinal ganglion cell loss does not abolish the scotopic threshold response (STR) of the cat and human ERG. *Clinical Vision Science* **2**, 149–158.

Sieving, P. A., Frishman, L. J. & Steinberg, R. H. (1986). Scotopic threshold response of proximal retina in cat. *Journal of Neurophysiology* **56**, 1049–1061.

Sieving, P. A. & Nino, C. (1988). Scotopic threshold response (STR) of the human electroretinogram. *Investigative Ophthalmology and Visual Science* **11**, 1608–1614.

Sieving, P. A. & Wakabayashi, K. (1991). Comparison of rod threshold ERG from monkey, cat and human. *Clinical Vision Science* **6**, 171–179.

Smith, R. G., Freed, M. A. & Sterling, P. (1986). Microcircuitry of the dark-adapted cat retina: functional architecture of the rod-cone network. *Journal of Neuroscience* **6**, 3505–3517.

Stockton, R. A. & Slaughter, M. M. (1989). B-Wave of the electroretinogram: a reflection of ON bipolar cell activity. *Journal of General Physiology* **93**, 101–122.

Toda, K., Bush, R. A., Humphries, P. & Sieving, P. A. (1999). The electroretinogram of the rhodopsin knockout mouse. *Visual Neuroscience* **16**, 391–398.

Tsukamoto, Y., Morigiwa, K., Ueda, M. & Sterling, P. (2001). Microcircuits for night vision in mouse retina. *Journal of Neuroscience* **2**, 8616–8623.

Viswanathan, S., Frishman, L. J., Robson, J. G., Harwerth, R. S. & Smith, E. L. III (1999). The photopic negative response of the macaque electroretinogram: reduction by experimental glaucoma. *Investigative Ophthalmology and Visual Science* **40**, 1124–1136.

Wyszecki, G. & Stiles W. S. (1982). *Color Science, Concepts and Methods, Quantitative Data and Formulae*, pp. 249–277. Wiley, New York.

Xu, X. J. & Karwoski, C. J. (1994). Current source density analysis of retinal field potentials. 2. Pharmacological analysis of the b-wave and m-wave. *Journal of Neurophysiology* **72**, 96–105.

Acknowledgements

We thank Josephine Wu for help with the experiments. The research was supported to by NIH grants T35 EY-07024, R01 EY06671, P30 EY07751, T31 EY07088.